



Tomas Bata University in Zlín
Library

Aluminum nanoparticles from liquid packaging board improve the competitiveness of (bio)diesel

Citation

MAROUŠEK, Josef. Aluminum nanoparticles from liquid packaging board improve the competitiveness of (bio)diesel. *Clean Technologies and Environmental Policy* [online]. Springer Nature, 2022, [cit. 2024-02-01]. ISSN 1618-954X. Available at <https://link.springer.com/article/10.1007/s10098-022-02413-y>

DOI

<https://doi.org/10.1007/s10098-022-02413-y>

Permanent link

<https://publikace.k.utb.cz/handle/10563/1011169>

This document is the Accepted Manuscript version of the article that can be shared via institutional repository.



TBU Publications

Repository of TBU Publications

publikace.k.utb.cz

Aluminum nanoparticles from liquid packaging board improve the competitiveness of (bio)diesel

Josef Maroušek^{1,2,3}

¹Institute of Technology and Business in České Budějovice, Faculty of Technology, Okružní 517/10, 370 01 Ceske Budejovice, Czech Republic

²Faculty of Agriculture and Technology, University of South Bohemia in České Budějovice, Studentská 1668, 370 05 Ceske Budejovice, Czech Republic

³Faculty of Management and Economics, Tomas Bata Univesity in Zlín, Mostní 5139, 760 01 Zlín, Czech Republic

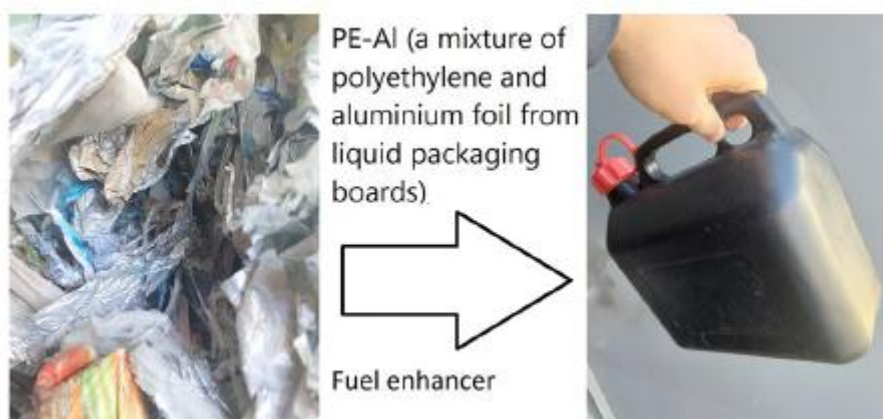
josef.marousek@gmail.com

Abstract

To date, no sustainable way of processing liquid packaging boards as a whole has been defined. The cardboard is occasionally recycled; however, there is no reliable demand for the resulting mixture of polyethylene and aluminum (*PE – Al*). Since Al leaching from landfills destroys both soil and water, it was proposed to prevent PE-Al landfilling by transforming *Al* into nanoparticles (*nAl*), which would be used as low-cost (bio)diesel additive. It is reported for the first time that the concept has been proved to be technically feasible and financially promising on a pilot scale. A series of tests with a single-cylinder water cooled combustion engine under various loading conditions revealed that the *nAl* obtained ($375.6 \text{ m}^2\text{g}^{-1}$) is capable of significantly increasing the reaction surface of the combustion process which manifests itself by (a) higher brake-specific fuel consumption, (b) enhanced brake thermal efficiency, and (c) significant drops in the production of combustion gases (*CO*; *HC*; *CO*₂ and *NO*_x in particular). Nevertheless, data indicate that there are untapped challenges regarding the presence of *O*₂ and further increasing the surface area of the *nAl*. Although the addition of *nAl* slightly reduced the oxidative stability and lubricity, these properties can be easily compensated by antioxidants and lubricants.

Keywords: PE-Al management, liquid packaging board, aluminum nanoparticles, biodiesel, circular economy

Graphical abstract



Introduction

Liquid packaging board (also known as multilayer packaging or TetraPak®) consists of laminated stiff paper (usually 65-80%), low density polyethylene (*LDPE*, in the range of 10-25%) and aluminum foil (*Al*, mostly between 3 and 10%). **Georgiopoulou et al. (2021)** estimated that over 160 countries are supplied with some 200 billion TetraPak® packages annually (not including local "non-branded" manufacturers). The paper from this waste can be recovered via composting (**Vochozka et al. 2017**), anaerobic fermentation (**Marousek, 2012**) or by washing out for the pulp industry (**Zawadiak et al. 2017**). There are also other alternatives, such as adding the recycled paper to building materials (**Martínez-Barrera et al. 2020**); low-quality plastic composites (**Martínez-Barrera et al. 2017**) and others (**Muo and Azeez, 2019**). However, what all these methods have in common is poor financial results (**Kliestik et al. 2018**) and the formation of a new type of challenging waste: a mixture of *HDPE* and *Al* (also known as *PE – Al*, **Fig. 1**). It was repeatedly reviewed that there have been countless attempts to divide *PE* from *Al* (**Xie et al. 2016**). Arguments why *PE – Al* incineration is environmentally and financially questionable were summarized and not disputed (**Streimikiene, 2021**). It is intuitive that pyrolysis of *PE – Al* faces similar difficulties (**Zúniga-Muro et al. 2020**). In short, there is no technology available on the market that is both environmentally friendly (**Kovacova et al. 2020**) and cost-effective (**Durana et al. 2021a**), therefore *PE – Al* is typically landfilled (**Skapa and Vochozka, 2019**). However, **Riaz et al. (2018)** demonstrated that similar practices creates preconditions for even more serious difficulties (**Durana et al. 2021b**), since *Al* is well known for its toxicity to plants and soil microorganisms (inhibition of root elongation, oxidative damage, disruption of cell organs, etc.).

At the same time, environmentally as well as economically driven efforts (**Novak et al. 2021**) are being made to substitute at least a part of fossil fuels (**Riley et al. 2021**). The US, Brazil and EU are among leading biodiesel producers (**Vochozka et al. 2020**), totaling some 40 Mt biodiesel annually (**Popescu et al. 2020**). It was repeatedly and independently confirmed that 1 L of biodiesel releases some 80% less *CO*₂; 50% less particulate emissions (*PM*); 20% less unburned hydrocarbons (*UHC*) and 10% less *CO* than conventional diesel (**Lakshmikandan et al. 2020**). However, despite long term and intensive efforts (**Valaskova et al. 2020**), combustion of biodiesel in compression-ignition (*CI*) engines results in higher emissions of nitrogen oxides (*NO*_x). To counteract the emission of *NO*_x, various technologies such as flue gas recirculation (**Sekar et al. 2021**); water stripping (**Manigandan et al. 2019**); addition of oxygenated fuels (methanol, ethanol and butanol); or nanoparticles (carbon nanotubes, ceramics, metal and metal oxides) are investigated (**Marousek et al. 2022**), whereas the nanoparticles of *Al* (*nAl*) and aluminum oxide (*nAl*₂O₃) seem to be the most promising (**Wu et al. 2018**).



Fig. 1 There are huge hills of *PE – Al* waste all around the globe for which no sustainable solution has yet been found (authors)

These nano-additives act as a combustion catalyst (an O₂ buffer with respect to NO_x) to advance the combustion performance and decrease pollutant emissions because of their multiple enhancement in thermophysical and chemical properties (higher porosity, reactivity, thermal conductivity, flash point, etc.). The exceptional properties of *nAl* and *nAl*₂O₃ are due to the fact that *Al* has a lower density and better thermal conductivity than most other metals (such as zinc, titanium and cerium oxides) which is beneficial for dispersion of its nanoparticles throughout the biodiesel and maintaining the stability of the suspension obtained (Manigandan et al. 2020). It was repeatedly and independently demonstrated that *nAl* addition to biodiesel increases surface/volume ratio which improves combustion characteristics, in particular by (a) reduction of the ignition delay and (b) enhancement of the fuel-air mixture (Nefzi, 2018). Although *nAl* or *nAl*₂O₃ are incorporated into biodiesel in the range of 20 to 200 ppm, this represents a significant additional cost (2,184.5 USD *Al t*⁻¹ and 85,400 USD *nAl t*⁻¹ as of March 15, 2021; London Metal Exchange). Such increased production costs represent a new challenge (Blazkova and Dvoulety, 2018) since biodiesel is so far cost competitive only under narrowly defined conditions (Kubalek et al. 2017). In other words, only if the following circumstances are met: (1) local diesel price is high (country is dependent on long-distance oil imports from problematic territories); (2) worthless feedstock is readily available (waste such as used and rancid oil or grease from sewage treatment plants) and (3) NO_x are lower than those of conventional diesel.

As soaring energy and fuel prices (even more than quadruple within 2 months in some EU Member states) have an overwhelming impact on global economy, there is an urgent need for alternative fuel sources, preferably of low environmental impact. The valorization of *Al* from liquid package boards into an additive for (bio)diesels would make it possible to transform (A) the environmental damage caused by *Al* landfilling into environmental benefits associated with lower exhaust gas production and (B) the economic losses associated with landfill fees into benefits associated with better (bio)diesel utilization.

Following the above, it is hypothesized whether the addition of *nAl* (made from *PE – Al*) to biodiesel might improve biodiesel characteristics in terms of *CI* engine performance and combustion gases. If this hypothesis is confirmed, it would make it possible to extend *PE – Al* waste management options and at the same time contribute to biodiesel competitiveness.

Table 1 Properties of Biodiesel and nano-additive blended fuel

Properties	Test Method	Diesel	MO	JO	JO+25 ppm	JO+50 ppm	MO+25 ppm	MO+50 ppm
Density (kg m ⁻³)	ASTMD4052	833	865	899	911	934	889	903
Kinematic Viscosity at 40 °C (mm ² s ⁻¹)	ASTMD4052	4.191	4.45	4.56	4.34	3.99	4.34	4.11
Cetane Number	ASTMD613	48.51	52.3	55.1	56.9	58.3	54.9	56.72
Calorific Value (KJ kg ⁻¹)	ASTDM240	42,969	43,175	44,322	46,001	46,822	44,211	45,021
Flash Point (°C)	ASTMD93	53	54	56	58	60	56	58
Ester content (%)	EN 14 103	–	97	97	97	97	97	97
Oxidative stability (h at 110 °C)	EN 14 112	–	8.1	7.3	7.3	7.3	8.1	8.1
Lubricity (µm)	HFFR	707	401	352	350	344	387	381

Materials and methods

nAl production

With the exception of analytical techniques, all reactants are of analytical purity. *PE – Al* was obtained from the JIP paper mill (Czech Republic, Fig. 1). The waste was added to (1:6 by weight) 4.2%

sodium hydroxide (NaOH) of industrial purity (PCC Group, Poland) and slowly stirred. After 2 h, the processing liquid was removed via a TMS017 screw 250 kN press (Aivotec Inc., Czech Republic) operating at maximum performance. Subsequently, the remaining *PE – Al* was added to 5% NaOH (1:5 by weight) and slowly stirred for 4 more hours (Sekar et al. 2021). Consequently, the processing liquid was removed for a second time using the TMS017 at 250 kN. The *PE* obtained was passed through RRR9 vibrating sieves (Pharmix Inc., Czech Republic) until humidity was reduced to below 5%. All the processing liquid obtained was mixed with 50% sulfuric acid (H₂SO₄) of industrial purity (Precheza, Czech Republic) until pH reached 4.0 (Lenhard et al. 2019). The precursor solution was slowly sun-dried in a 2 cm layer until the moisture was reduced to 5%. „Al was subsequently synthesized by the sol-gel method (Radhakrishnan et al. 2018). Initially, the precursor solution was subjected to hydrolysis for 24 h to prepare the sol. Afterward, the sol was stirred for 48 h and dried at 110 °C. Once the xerogel was obtained, sintering was carried out at 1100 °C for the formation of „Al (properties stated in Table 1).

Table 2 Physical-chemical characteristics of kitchen oil

	Value	Unit
Iodine number	79.7 ± 4.5	gI ₂ 100 g ⁻¹
Acid value	4.0 ± 0.6	mg KOH g ⁻¹
Peroxide value	25.9 ± 3.4	mg kg ⁻¹
Saponification	108.3 ± 34.1	mg KOH g ⁻¹
Viscosity (40 °C; 50 °C; 60 °C)	4.9 ± 1.1; 4.3 ± 0.9; 4.0 ± 0.9	mm ² s ⁻¹
Density	0.93 ± 0.13	kg L ⁻¹
Free water	6.2 ± 0.5	g kg ⁻¹
Solid impurities	37.4 ± 18.9	g kg ⁻¹

Table 3 Physical-chemical characteristics of grease

	Value	Unit
Free fatty acids	170.6 ± 24.5	g kg ⁻¹
Viscosity (60 °C)	185.7 ± 13.8	mm ² s ⁻¹
Density	0.91 ± 0.03	kg L ⁻¹
Free water	225.9 ± 33.7	g kg ⁻¹
Solid impurities	293.4 ± 80.1	g kg ⁻¹

Biodiesel production

Used kitchen oil (origin was investigated via electronic questionnaire) was obtained from the local waste collection system. Grease was obtained from the local sewage treatment plant. Physical-chemical characteristics of both raw materials are provided in Tables 2 and 3. Both feedstocks were heated to 70 °C and passed through a refining process to remove impurities (refined used kitchen oil (*MO*); refined grease (*JO*)). Hot oils were subsequently subjected to transesterification according to

established methods (Hadzima et al. 2007), where both NaOH (PCC Group, Poland) and methanol (CH₃OH; Methanex, Belgium) were of industrial purity to better simulate the commercial scale procedures (Novakova et al. 2022). After settling for 24 h the glycerol (C₃H₈O₃) was decanted from the bottom and traces of CH₃OH were removed by distillation (65 °C).

Table 4 Physical properties of *nAl*

Alumina color	White
Specific surface area	375.6 ± 12.9 (m ² g ⁻¹)
Bulk density	0.173 ± 0.035 (gcm ⁻³)
Average particle size (95% distribution)	25 up to 30 nm

The biodiesels obtained (used kitchen oil-based biodiesel (*MB*) and sewage treatment plant grease-based biodiesel (*JO*)) were enriched with *nAl* (prepared as in Sect. 2.1) using a UP400S ultrasonic homogenizer (Hielscher Ultrasonics, Germany) at 24 kHz for 40 min to respect the financial point of view (Wagner et al. 2021). The properties of the enriched biodiesels are given in Table 4.

Engine setup

All the tests were conducted using the single-cylinder, air-cooled, four-stroke unmodified 4.3 kW (1500 rpm) Kirloskar-AV1 engine (Kirloskar Group, India) that is designed for the techno-economic analysis of fuel performance (Rowland et al. 2021). The samples were as follows: 1/100% diesel fuel; 2/30% *MB* and 70% diesel; 3/30% *JO* and 70% diesel; 4/(2) + 25 ppm *nAl*; 5/(2) + 50 ppm *nAl*; 6/ (3) + 25 ppm *nAl* and 7/(3) + 50 ppm *nAl*, respectively. To observe the emission values, a M.O.V.E GAS PEMS portable exhaust gas analyzer (AVL, Austria) was fitted to the engine model. Sensors were linked to the data acquisition system to track the changes in the (a) fuel flow rate; (b) engine load; (c) emission rate; (d) cylinder temperature and (e) pressure (Dorskocil et al. 2016). Furthermore, a *K*-type (0 to 1200 °C) thermocouple was used to determine the temperatures in the exhaust gas pipe and combustion chamber. The loads are provided to the engine with the aid of a TASI7 dynamometer (Sierra, USA). Meanwhile, the consumption of the fuel is measured using a fuel measuring burette. All the data were processed using a 6218 USB data acquisition system (National Instruments, USA). A simplified layout of the experiment setup is shown in Fig. 2.

Uncertainty analysis

The basic equation for finding the rate of errors and uncertainties was

$$F = F(X_1, X_2, X_3 \dots X_n) \quad (1)$$

where *F* denotes the final error during the observation obtained from various instruments.

All tests were conducted with a minimum of 6 cycles and the average values were obtained for the final representation. Before running each blend, the engine was allowed to idle for at least 5 min using neat diesel fuel.

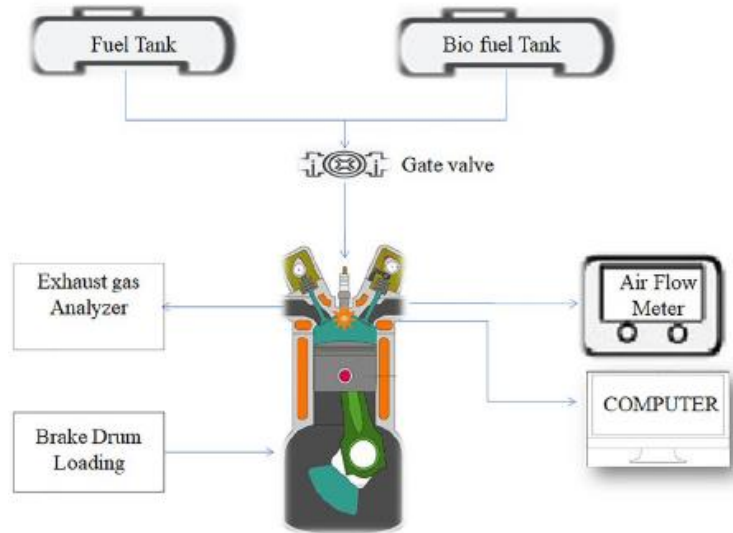


Fig. 2 Schematic layout of the experimental setup

$$\frac{U_F}{F} = \sqrt{\left(\frac{X_n \partial F}{F \partial X_n}\right)^2 \frac{U_{X_n}^2}{X_n^2}} \quad (2)$$

Results and discussion

Feedstock characteristics

Electronic questionnaire revealed that origin of the kitchen oil is as follows: rapeseed oil (54%); sunflower oil (19%); animal fats (11%) and olive oil (10%). Su, a distribution of oils in good agreement with **Nefzi (2018)**, who reported that European cuisine is dominated by sunflower and rapeseed oils, whereas North American cuisine is dominated by soybean oil, and in Asia palm oil plays a major role (followed by animal fats). Summary of the key physical and chemical characteristics (**Table 2**) indicates that is a common sample of cooking oils that are common in Europe. The only exception is the increased number of solid impurities, which is probably due to the specifics of the local cuisine (the high popularity of Wiener Schnitzel). Characteristics of grease are provided in **Table 3**. The values obtained can be interpreted that it was the usual grease from the sewage treatment plant.

Combustion characteristics

Engine performance is usually assessed using the cetane number, fuel/air blending rate and the viscous nature of the fuel since these indicators have an easy commercial interpretation.

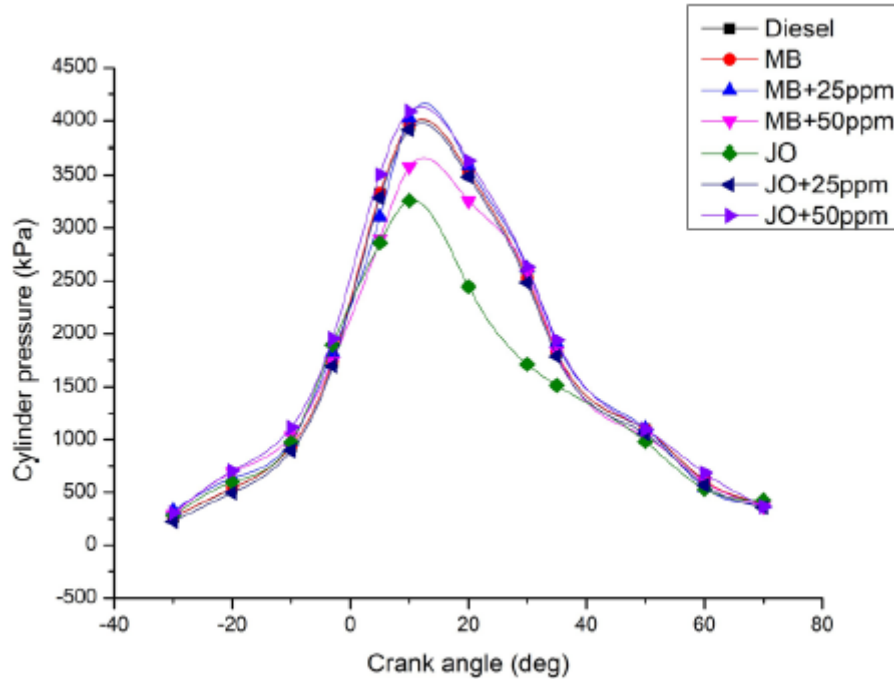


Fig. 3 Variation of in-cylinder pressure at full load

During the *CI* process, maximum cylinder pressure can be indirectly determined via the percentage of burnt fuel. **Figure 3** depicts the cylinder performance at full load with different fuel blends. All biodiesel blends showed similar performance at 100% load. The peak cylinder pressures of *MB*, *JO* and diesel were 4050 kPa, 4060 kPa and 3420 kPa, respectively. On the other hand, the maximum peak pressure reported by the blend of *MB* + 25 ppm *nAl* and the minimum peak pressure of *JO* blends were 3990 kPa and 3112 kPa. The non-uniform combustion characteristics of the fuels make it difficult to control engine power and can cause damage to the cylinder (**Jandacka et al. 2017**). All the biodiesel blends resulted in higher cylinder pressures than the neat diesel due to the incomplete combustion process. Further, the calorific value of the biodiesel is another vital reason for the higher cylinder pressure values (**Streimikiene 2020**). Data visualization reveals that incorporation of *nAl* improves the cylinder pressure significantly along with enhanced thermal conductivity. Addition of varying concentrations of *nAl* at 25 ppm and 50 ppm enhances the cylinder peak pressure. According to existing literature this enhancement of the combustion process by adding nanoparticles follows two linked mechanisms. First, the biodiesel blends chemical structure breaks and adheres well with nanoparticles (**Vo et al. 2020**). Secondly, the good binding nature of the biodiesel with the nanoparticles enhances the rate of reaction. During the combustion reaction, the O_2 molecules are liberated easily from the *nAl*. The *UHC* present at the surfaces of the piston interfaces reacts with the liberated O_2 molecules present in *nAl*. Increasing the concentration of *nAl* produces extra O_2 molecules and the percentage of hydrocarbon emission reduces by means of the extra O_2 molecules. Maximum cylinder peak pressure was achieved during the combustion process due to an increase in the proportion of nanoparticles.

The combustion process onsets earlier in biodiesel blends due to higher proportions of *nAl*, as is evident in **Fig. 3**. In addition, increased concentrations of *nAl* enhance the thermal conductivity and ignition reaction quality. **Manigandan et al. (2019)** used moringa seed biodiesel and a high peak pressure of 4150 kPa was observed at a crank angle of 3°. This was achieved by adding soluble multi-walled carbon nanotubes. It can therefore be concluded that an improvement in thermal conductivity and an enhancement of ignition behavior was observed due to the addition of *nAl*.

Figure 4 depicts the heat release rate of nanoparticle incorporated biodiesel blends and a comparison with diesel and pure biodiesel blends. A maximum heat release rate of 34 J deg CA^{-1} (crank angle) was observed in the *JO* blend. *MB* + 25 ppm and *JO* + 25 ppm blends exhibit heat release rate values of 29 J deg CA^{-1} and 26 J Deg CA^{-1} , respectively. More heat generation and higher calorific value contribute to a high heat release rate during the combustion mechanism. Incorporation of *nAl* at higher concentration enhances the heat release rate to a higher level and thereby improves the thermal conductivity and quality of the ignition mechanism (Vochozka et al. 2016).

Brake-specific fuel consumption

Brake-specific fuel consumption (*BSFC*) is generally defined as the quantity of fuel consumed by an engine to produce 1 kW of energy (Dzhalladova et al. 2019). The *BSFC* of different biodiesel, diesel and *nAl* incorporated biodiesel blends is depicted in Fig. 5 based on different load conditions. It is evident that the high energy consumption of the engine to maintain a steady speed was caused by a decreased *BSFC* value at 100% load. The *BSFC* of *JO* and *MB* showed 16% to 18% higher values than with neat diesel fuel. The heating value of biodiesel is less than that of diesel blends, which increases the consumption of biodiesel (Bartos et al. 2021).

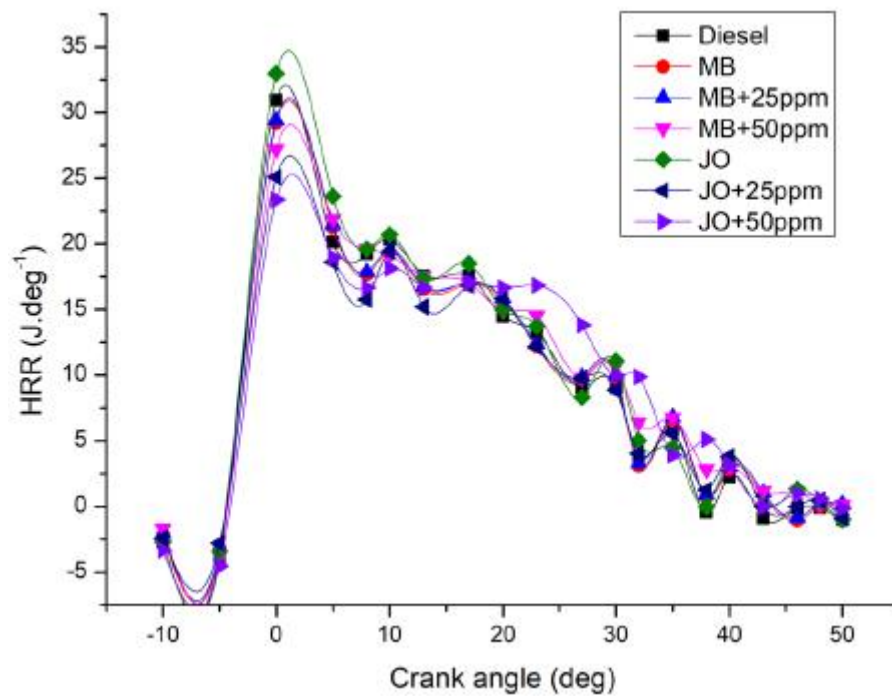


Fig. 4 Heat release rate at full load

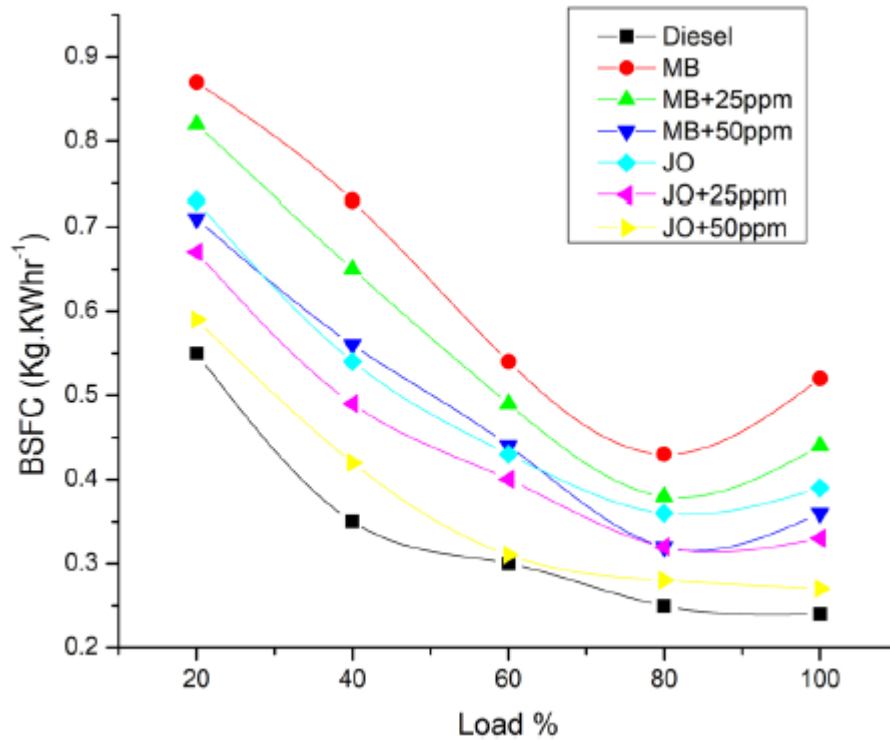


Fig. 5 BSFC of various biodiesel blends under varying loads

The BSFC values of JO and MB were found to be 0.87 and 0.73 kg kWh⁻¹, respectively, at 20% load. These values were compared with neat diesel, JO and MB were 45.3% and 39.4%, respectively, increases the BSFC values. Further decreases in the BSFC values of JO and MB were found due to the addition of *nAl*. At 40% load, the addition of 50 ppm *nAl* to JO and MB reduces the brake-specific fuel consumption by 22.3% and 22.2%, respectively, whereas incorporation of 25 ppm of *nAl* to JO and MB reduces specific fuel consumption by 10.9% and 8.5%, respectively. The combustion mechanism was enhanced significantly due to *nAl* addition, and this is mainly due to extra available O₂ content in *nAl* and also in biodiesel. The BSFC values of JO were found to be higher than for the other biodiesel blends.

Brake thermal efficiency

Brake thermal efficiency (BTE) is typically defined as the mechanical energy converted from the heat fuel energy in an efficient manner. The brake thermal efficiency of both biodiesel blends, pure diesel and *nAl*-enriched biodiesels is shown in Fig. 6 for different load regimes. Pure biodiesels and diesel showed lower and higher BTE values, respectively. Similar to BSFC, addition of *nAl* enhances the BTE values significantly due to the presence of extra O₂ and the excess O₂ acts as a catalyst to improve the fuel consumption efficiency. Addition of 50 ppm and 25 ppm of *nAl* improves the BTE values of MB and JO by 2.1% and 3.9%, respectively, compared to pure biodiesel. At 60% load the BTE of diesel, MB and JO were 29%, 17.5% and 23.2%, respectively. The efficiency of MB and JO showed 5.8% and 11.5% reduction in values compared to neat diesel fuel. At 80% load BTE values of 50 ppm of *nAl* incorporated JO specimens showed a value 1.1% higher than diesel. The BTE value of JO enhanced by 50 ppm of *nAl* exhibits similar values of conventional diesel at full load (Sekar et al. 2021).

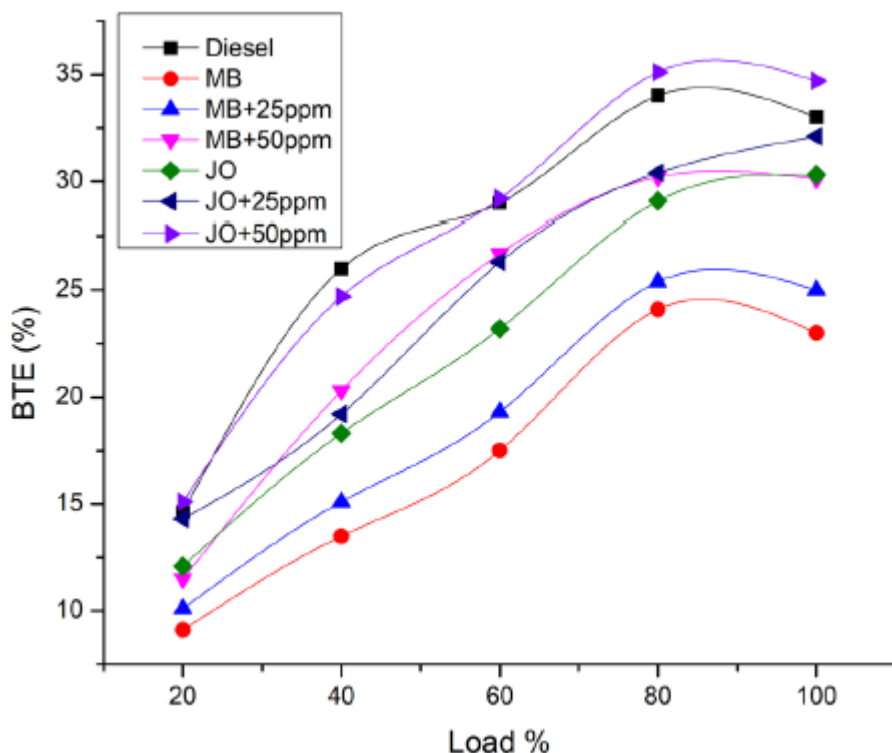


Fig. 6 BTE of various biodiesel blends under varying loads

Emission characteristics

The carbon monoxide (CO) emissions released from diesel, biodiesels and nAl -enriched biodiesel blends with two different concentrations are depicted in **Fig. 7** under varying load regimes (**Manigandan et al. 2019**). Following the combustion of MB and JO , CO emissions were 17.7% and 24.3%, respectively, which is lower than for pure diesel. Maximum CO emissions occurred at 100% load for all the fuel samples.

At full load, the CO emission of diesel; MB ; JO ; $MB + 25 \text{ ppm } nAl$, $MB + 50 \text{ ppm } nAl$; $JO + 25 \text{ ppm } nAl$ and $JO + 50 \text{ ppm } nAl$ were 0.125; 0.09; 0.091; 0.077; 0.066; 0.082 and 0.079, respectively. The mixtures enriched with 50 ppm of nAl showed better performance than all the other fuels. The 100% biodiesel fuels exhibit lower CO emissions than neat diesel (**Tvaronaviciene et al. 2018**). Reduction in CO emission concentration has significant environmental benefits (**Marousek and Trakal 2022**). Emission of CO is mainly attributed to incomplete oxidation. In other words, better oxidation results in a significant reduction of CO emissions. The production of CO was mitigated by the presence of additional O_2 in the biodiesel, which enhances the formation of CO_2 instead of CO . There are several factors which influence CO formation including the temperature of the interfacial region, the O_2 content of the fuel, the alcohol percentage and the spray characteristics of the fuel (**Jandacka et al. 2017**). At higher loads, CO emission concentration was significantly higher than other load conditions. This is attributed to the higher consumption of fuel at higher loads during the combustion mechanism and the fuel is much richer than in other load regimes, resulting in higher CO emissions (**Sekar et al. 2021**). Incorporation of nAl provides additional O_2 molecules and further reduces CO emissions due to the formation of CO_2 (**Marousek 2022**).

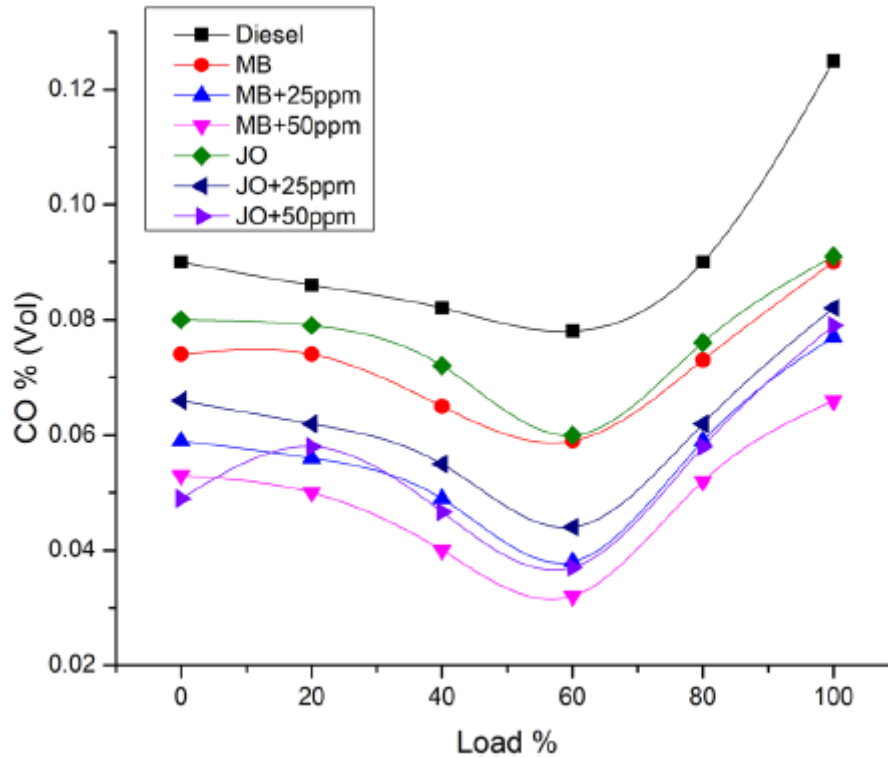


Fig. 7 CO emissions of various biodiesel blends under varying loads

Emission of NO_x following the use of diesel, biodiesels and nAl -enriched biodiesels at varying load regimes is depicted in Fig. 8. According to Jandacka et al. (2017) the presence of O_2 in the atmosphere at higher altitudes combines with the nitrogen emitted during the combustion mechanism, resulting in the formation of NO_x . The formation of NO_x is also favored at higher temperatures. The NO_x emissions were considerably higher at full load regimes for diesel, biodiesels and nAl -enriched biodiesel blends. From Fig. 8 it can be seen that conventional diesel exhibits lower NO_x emissions than the other fuels. A similar trend was reported in the literature (Vo 2020). Enhancement of the cetane number was observed with the addition of nAl in higher concentrations. As the concentration of the nanoparticles increases, the properties of the fuel were improved, especially the cetane and calorific values. This enhancement considerably reduces the NO_x emission into the atmosphere at all load regimes. AlO molecules were formed at high temperature and the chance of NO_x generation is considerably less which leaves N_2 molecules during the reaction of NO_x and Al_2O_3 . NO_x emissions of diesel; MB; MB + 25 ppm nAl ; MB + 50 ppm nAl ; JO + 25 ppm nAl and JO + 50 ppm nAl were 191; 278; 223; 243; 212; 201 and 178, respectively, at 0% load. At full load, MB and JO exhibit 41.6% and 15.3% higher NO_x values than diesel fuel. Addition of nAl with 25 ppm and 50 ppm concentrations reduces the NO_x emission of 100% MB by 12.5% and 21.1%, respectively. Inclusion of 50 ppm nAl to MB and JO showed better results than other fuel samples.

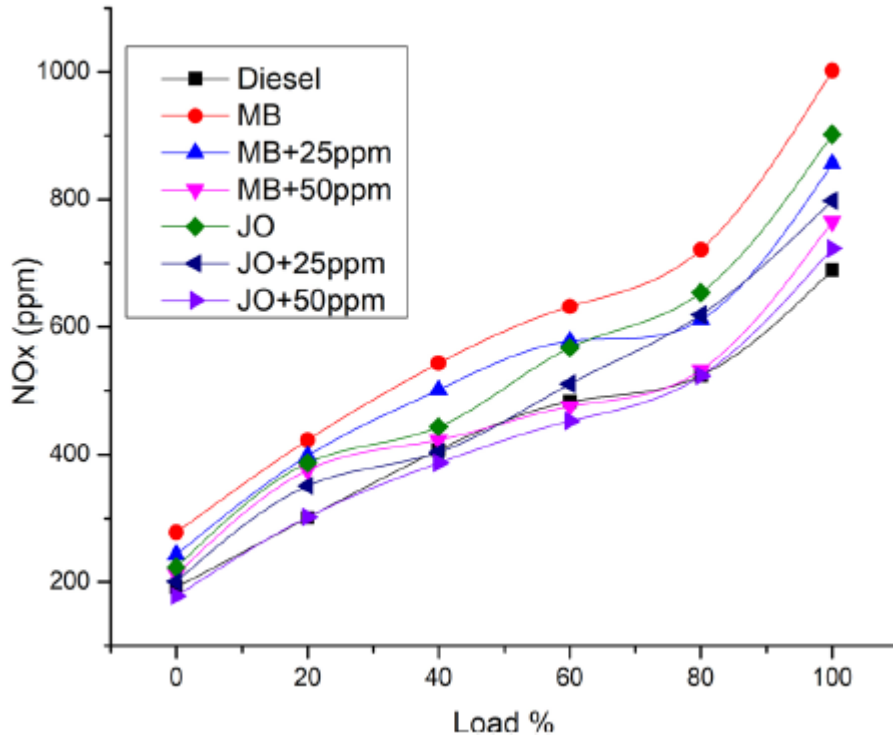


Fig. 8 NO_x emissions of various biodiesel blends under varying loads

The concentration of *UHC* emissions following the combustion of diesel, biodiesels and *nAl*-enriched biodiesel blends with two different concentrations is depicted in Fig. 9 at varying load regimes. In the case of a *CI* engine, the level of *UHC* was high. The factors influencing the *UHC* include the interface of the piston, leftover fuel in the nozzle region and cervical surface. Some other factors of *UHC* formation are incomplete fuel evaporation, spray infringement and the interfacial region between the cylinder wall and the liquid. The concentrations of *UHC* emissions were significantly higher at 100% load due to the high consumption of fuels during the combustion mechanism and this is shown in Fig. 9. The concentration of *UHC* was very low for biodiesels with 50 ppm *nAl*. Diesel fuel showed higher *UHC* levels than *MB* and *JO* (Zavadsky et al. 2019). The *UHC* emission concentration of 100% *MB* and *JO* was 10.7% and 14.5% lower, respectively, than diesel fuel at the 40% load regime. Similar to *CO* emissions, the presence of additional O₂ reduces the *UHC* emissions due to the incorporation of „Al. Addition of „Al forms lean biodiesel blends and further improves the thermal conductivity and combustion process, thereby decreasing the *UHC* concentration. *UHC* emissions were suppressed by improving the combustion process by adding higher dosages of „Al. Of the various biodiesel mixtures, those enriched with 50 ppm of „Al showed better results in terms of reducing the NO_x, *CO* and *UHC* emissions. Based on the average values, the total contribution of the error was 2.54% and this is within the permissible limits.

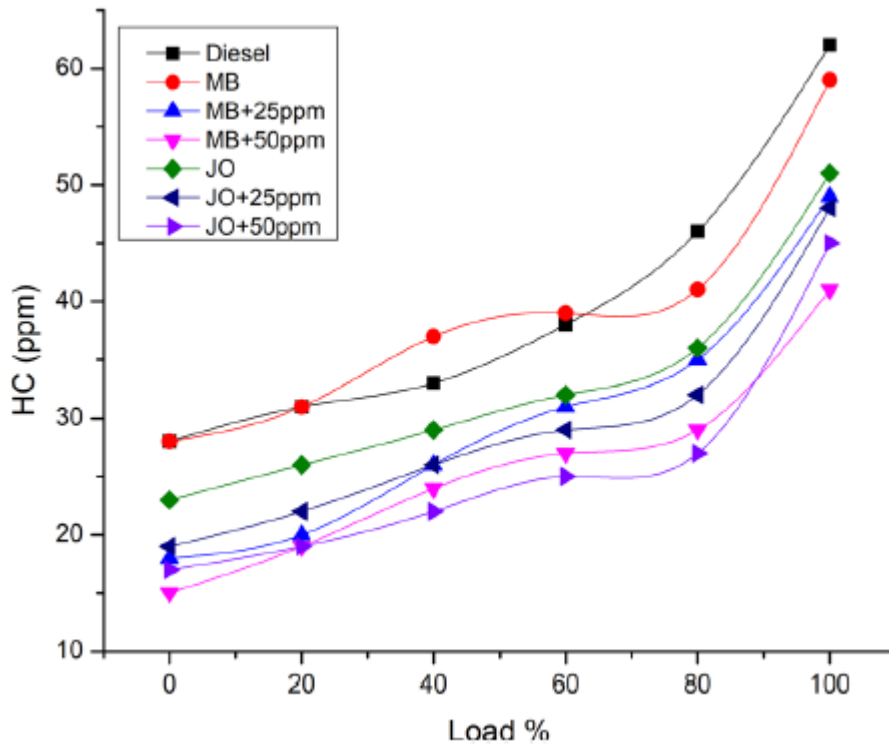


Fig. 9 HC emissions of various biodiesel blends under varying loads

Conclusion

It is possible to produce functional „Al out of PE – Al waste. The *BSFC* of *JO* and *MB* showed higher values than for neat diesel fuel. At 40% load, *JO* and *MB* enriched with 50 ppm of „Al reduces the *BSFC* by 22% and 22%, respectively, whereas enrichment with only 25 ppm of „Al reduces the *BSFC* by 11% and 9%, respectively. Pure biodiesels and diesel showed lower and higher *BTE* values, respectively. Similar to *BSFC*, addition of „Al enhances the *BTE* values significantly due to the presence of extra O_2 which simultaneously acts as a catalyst. At 80% load *BTE* values of *JO* enriched with 50 ppm „Al showed a 1.1% higher value than diesel. The *BTE* value of *JO* enriched with 50 ppm „Al exhibits similar values to conventional diesel at full load.

With regard to the emissions, biodiesel blends reported lower emissions than for neat diesel. The main reason for the reduction of CO , NO_x and HC was due to the heating values and the complete combustion process. The formation of NO_x was also favored by the higher temperature. The NO_x emissions were considerably higher at the full load regimes for the diesel, biodiesel and „Al addition biodiesel blends. Conventional diesel exhibits lower NO_x emissions than the other diesel blends. Enhancement of the cetane number was observed with the addition of „Al at higher concentrations. Of the various biodiesel mixes, the samples with 50 ppm showed better results in terms of reducing NO_x , CO and UHC .

References

Bartos V, Vochozka M, Janikova J (2021) Fair value in squeeze-out of large mining companies. Acta Montanistica Slovaca 26(4). [https:// doi.org/10.46544/AMS.v26i4.10](https://doi.org/10.46544/AMS.v26i4.10)

- Blazkova I, Dvoulety O (2018) Sectoral and firm-level determinants of profitability: a multilevel approach. *Int J Entrep Knowl* 6(2):32-44. <https://doi.org/10.2478/IJEK-2018-0012>
- Doskocil R, Skapa S, Olsova P (2016) Success evaluation model for project management. *Econ Manag* 19(4):167-185. <https://doi.org/10.15240/tul/001/2016-4-012>
- Durana P, Michalkova L, Privara A, Marousek J, Tumpach M (2021a) Does the life cycle affect earnings management and bankruptcy? *Oecon Copernic* 12(2):425-461
- Durana P, Perkins N, Valaskova K (2021b) Artificial intelligence data-driven internet of things systems, real-time advanced analytics, and cyber-physical production networks in sustainable smart manufacturing. *Econ Manag Financ Mark* 16:20-30
- Dzhalladova I, Skapa S, Novotna V, Babynyuk A (2019) Design and analysis of a model for detection of information attacks in computer networks. *Econ Comput Econ Cybern Stud Res*. <https://doi.org/10.24818/18423264/53.3.19.06>
- Georgiopoulou I, Pappa GD, Vouyiouka SN, Magoulas K (2021) Recycling of post-consumer multilayer Tetra Pak® packaging with the Selective Dissolution-Precipitation process. *Resour Conserv Recycl* 165:105268
- Hadzima B, Janecek M, Estrin Y, Kim HS (2007) Microstructure and corrosion properties of ultrafine-grained interstitial free steel. *Mater Sci Eng, A* 462(1-2):243-247
- Jandacka J, Micieta J, Holubcik M, Nosek R (2017) Experimental determination of bed temperatures during wood pellet combustion. *Energy Fuels* 31(3):2919-2926
- Kliestik T, Misankova M, Valaskova K, Svabova L (2018) Bankruptcy prevention: new effort to reflect on legal and social changes. *Sci Eng Ethics* 24(2):791-803
- Kovacova M, Segers C, Tumpach M, Michalkova L (2020) Big data-driven smart manufacturing: sustainable production processes, real-time sensor networks, and industrial value creation. *Econ Manag Financ Mark* 15(1):54-61
- Kubalek J, Camska D, Strouhal J (2017) Personal bankruptcies from macroeconomic perspective. *Int J Entrep Knowl*. <https://doi.org/10.37335/ijek.v5i2.61>
- Lakshmikandan M, Murugesan AG, Wang S, Abomohra AEF, Jovita PA, Kiruthiga S (2020) Sustainable biomass production under CO2 conditions and effective wet microalgae lipid extraction for biodiesel production. *J Clean Prod* 247:119398
- Lenhard R, Malcho M, Jandačka J (2019) Modelling of heat transfer in the evaporator and condenser of the working fluid in the heat pipe. *Heat Transfer Eng* 40(3-4):215-226
- Manigandan S, Gunasekar P, Devipriya J, Nithya S (2019) Emission and injection characteristics of corn biodiesel blends in diesel engine. *Fuel* 235:723-735. <https://doi.org/10.1016/j.fuel.2018.08.071>
- Manigandan S, Atabani AE, Ponnusamy VK, Pugazhendhi A, Gunasekar P, Prakash S (2020) Effect of hydrogen and multiwall carbon nanotubes blends on combustion performance and emission of diesel engine using Taguchi approach. *Fuel* 276:118120. <https://doi.org/10.1016/j.fuel.2020.118120>
- Marousek J (2012) Finding the optimal parameters for the steam explosion process of hay. *Revista Técnica De La Facultad De Ingeniería Universidad Del Zulia* 35:170-178
- Marousek J, Strunecky O, Bartos V, Vochozka M (2022) Revisiting competitiveness of hydrogen and algae biodiesel. *Fuel* 328:125317

Marousek J, Trakal L (2022) Techno-economic analysis reveals the untapped potential of wood biochar. *Chemosphere* 291:133000 Marousek J (2022) Nanoparticles can change (bio) hydrogen competitiveness. *Fuel* 328:125318

Martínez-Barrera G, Martínez-Lopez M, Gonzalez-Rivas N, del Coz-Díaz JJ, Avila-Cordoba L, dos Reis JML, Gencel O (2017) Recycled cellulose from Tetra Pak packaging as reinforcement of polyester based composites. *Constr Build Mater* 157:1018-1023

Martínez-Barrera G, del Coz-Díaz JJ, Alonso-Martínez M, Martínez-López M (2020) Lamellae of waste beverage packaging (Tetra Pak) and gamma radiation as tools for improvement of concrete. *Case Stud Construct Mater* 12:e00315

Muo I, Azeez A (2019) Green entrepreneurship: literature review and agenda for future research. *Int J Entrep Knowl* 7(2):17-29. <https://doi.org/10.37335/ijek.v7i2.90>

Nefzi N (2018) Fear of failure and entrepreneurial risk perception Fear of Failure and Entrepreneurial Risk Perception. *Int J Entrep Knowl* 6(2):45-58. <https://doi.org/10.2478/ijek-2018-0013>

Novak A, Bennett D, Kliestik T (2021) Product decision-making information systems, real-time sensor networks, and artificial intelligence-driven big data analytics in sustainable industry 4.0. *Econ Manag Financ Mark* 16(2):62-72

Novakova L, Novotna L, Prochazkova M (2022) Predicted future development of imperfect complementary goods-copper and zinc until 2030. *Acta Montanistica Slovaca* 135-151. <https://doi.org/10.46544/AMS.v27i1.10>

Popescu GH, Zvarikova K, Machova V, Mihai EA (2020) Industrial big data, automated production systems, and Internet of Things sensing networks in cyber-physical system-based manufacturing. *J Self-Gov Manag Econ* 8(3):30-36

Radhakrishnan S, Munuswamy DB, Devarajan Y, Mahalingam A (2018) Effect of nanoparticle on emission and performance characteristics of a diesel engine fueled with cashew nut shell biodiesel. *Energy Sources Part A Recov Util Environ Eff* 40(20):2485-2493

Riaz M, Yan L, Wu X, Hussain S, Aziz O, Imran M, Jiang C (2018) Boron reduces aluminum-induced growth inhibition, oxidative damage and alterations in the cell wall components in the roots of trifoliolate orange. *Ecotoxicol Environ Saf* 153:107-115

Riley C, Vrbka J, Rowland Z (2021) Internet of things-enabled sustainability, big data-driven decision-making processes, and digitized mass production in industry 4.0-based manufacturing systems. *J Self-Gov Manag Econ* 9:42-52

Sekar M, Kumar TP, Kumar MSG, Vanickova R, Marousek J (2021) Techno-economic review on short-term anthropogenic emissions of air pollutants and particulate matter. *Fuel* 305:121544

Skapa S, Vochozka M (2019) Waste energy recovery improves price competitiveness of artificial forage from rapeseed straw. *Clean Technol Environ Policy* 21(5):1165-1171

Streimikiene D (2020) Ranking of Baltic States on progress towards the main energy security goals of European energy union strategy. *J Int Stud* 13(4):24-37. <https://doi.org/10.14254/2071-8330.2020/13-4/2>

Streimikiene D (2021) Externalities of power generation in Visegrad countries and their integration through support of renewables. *Econ Sociol* 14(1):89-102. <https://doi.org/10.14254/2071-789X.2021/14-1/6>

Tvaronavičienė M, Prakapienė D, Garškaitė-Milvydienė K, Prakapas R, Nawrot L (2018) Energy efficiency in the long-run in the selected European countries. *Econ Sociol* 11(1):245-254. <https://doi.org/10.14254/2071-789X.2018/11-1/16>

Rowland Z, Blahova A, Peng, GAO (2021) Silver as a value keeper and wealth distributor during an economic recession. *Acta Mon-tanistica Slovaca* 26(4). <https://doi.org/10.46544/AMS.v26i4.16>

Valaskova K, Throne O, Kral P, Michalkova L (2020) Deep learning-enabled smart process planning in cyber-physical system-based manufacturing. *J Self-Gov Manage Econ* 8(1):121-127

Vo HD (2020) Sustainable agriculture and energy in the US: A link between ethanol production and the acreage for corn. *Econ Sociol* 13(3):259-268. <https://doi.org/10.14254/2071-789X.2020/13-3/16>

Vochozka M, Marouskova A, Vachal J, Strakova J (2016) Reengineering the paper mill waste management. *Clean Technol Environ Policy* 18(1):323-329

Vochozka M, Marousková A, Suler P (2017) Obsolete laws: economic and moral aspects, case study—composting standards. *Sci Eng Ethics* 23(6):1667-1672

Vochozka M, Rowland Z, Suler P, Marousek J (2020) The influence of the international price of oil on the value of the EUR/USD exchange rate. *J Compet* 12(2):167

Wagner J, Petera P, Popesko B, Novak P, Šafr K (2021) Usefulness of the budget: the mediating effect of participative budgeting and budget-based evaluation and rewarding. *Balt J Manag* 16(4):602-620

Wu Q, Xie X, Wang Y, Roskilly T (2018) Effect of carbon coated aluminum nanoparticles as additive to biodiesel-diesel blends on performance and emission characteristics of diesel engine. *Appl Energy* 221:597-604

Xie M, Bai W, Bai L, Sun X, Lu Q, Yan D, Qiao Q (2016) Life cycle assessment of the recycling of Al-PE (a laminated foil made from polyethylene and aluminum foil) composite packaging waste. *J Clean Prod* 112:4430-4434

Zavadsky J, Korenkova V, Zavadska Z, Kadarova J, Tucek D (2019) Competences in the quality management system evaluation based on the most worldwide used key performance indicators. *Calitatea* 20(169):29-41

Zawadiak J, Wojciechowski S, Piotrowski T, Krypa A (2017) Tetra pak recycling-current trends and new developments. *Am J Chem Eng* 5(3):37-42

Zúñiga-Muro NM, Bonilla-Petriciolet A, Mendoza-Castillo DI, Duran-Valle CJ, Silvestre-Albero J, Reynel-Ávila HE, Tapia-Picazo JC (2020) Recycling of Tetra pak wastes via pyrolysis: Characterization of solid products and application of the resulting char in the adsorption of mercury from water. *J Clean Prod* 291:125219